CrossMark

ORIGINAL ARTICLE

Additive manufacturing methods and modelling approaches: a critical review

H. Bikas[1] · P. Stavropoulos[1,2] · G. Chryssolouris[1]

Abstract Additive manufacturing is a technology rapidly expanding on a number of industrial sectors. It provides design freedom and environmental/ecological advantages. It transforms essentially design files to fully functional products. However, it is still hampered by low productivity, poor quality and uncertainty of final part mechanical properties. The root cause of undesired effects lies in the control aspects of the process. Optimization is difficult due to limited modelling approaches. Physical phenomena associated with additive manufacturing processes are complex, including melting/solidification and vaporization, heat and mass transfer etc. The goal of the current study is to map available additive manufacturing methods based on their process mechanisms, review modelling approaches based on modelling methods and identify research gaps. Later sections of the study review implications for closed-loop control of the process.

Keywords Additive manufacturing · Process control · Process mechanisms · Modelling methods

1 Introduction

Additive manufacturing (AM) is defined as "the process of joining materials to make objects from 3D model data, usually

✉ G. Chryssolouris
    xrisol@lms.mech.upatras.gr

[1] Laboratory for Manufacturing Systems and Automation, Department of Mechanical Engineering and Aeronautics, University of Patras, Patras 265 00, Greece

[2] Department of Aeronautical Studies, Hellenic Air Force Academy, Dekelia Air-Force Base, TGA 1010 Athens, Greece

layer upon layer, as opposed to subtractive manufacturing methodologies, such as traditional machining" [1]. AM can deliver parts of very intricate and complex geometries with a minimum need for post-processing, built from tailored materials with near-zero material waste, while being applicable to a variety of materials, including plastics and metals. Therefore, AM is a tool that offers increased "design freedom" and enables designers and engineers to create unique products that can be manufactured at low volumes in an economical way. An indicative example of the design freedom offered is that conventional assemblies can be redesigned in a single complex structure that could not be manufactured with the current manufacturing processes. Another driver of the AM technology is that it is environmentally and ecologically promising. Additive manufacturing technologies and methods are increasing constantly in terms of application and market share, spreading into various manufacturing divisions, such as automotive, medical and aerospace, and are expected that this heavy growth will continue over the next few years. According to the Gartner report [2], sales of sub-$100,000 AM machines have grown worldwide by 49 % in 2014 and are expected to have reached a 75 % growth rate by the end of 2014.

In terms of materials processed, plastics are currently leading the AM market, with around 30,000 machines in production [3]; however, the metal AM market is also growing. With over 1500 machines sold to date (Fig. 1), it is expected that the metal AM machines will see double-digit percentage growth in their sales, over the next 5 years, despite the global recession.

Indeed, according to [5], the industry's average annual growth (CAGR) over the past 25 years is impressive, namely 25.4 % (Figs. 2 and 3).

In the last few years, there is a significant trend towards metal AM for the production of structural components, mainly in areas, such as aerospace and motorsport applications, that
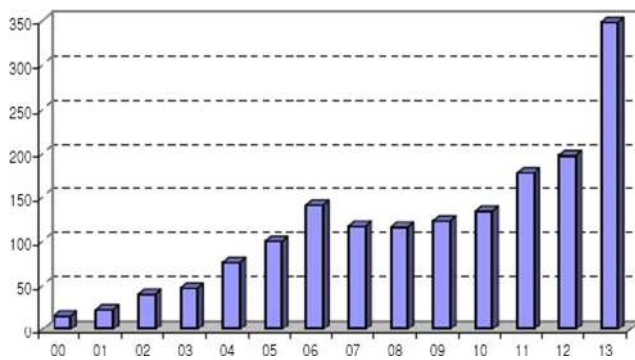
Fig. 1 Metal AM machine annual sales (Wohlers report 2014) [4]

could benefit from significant weight savings. A lot of effort is being made on making those AM processes faster and more reliable. Therefore, the modelling of metal AM processes is a "hot topic" as it is the main enabler for process (and product) optimization.

2 Additive manufacturing methods

A large number of additive manufacturing processes are now available; they differ in the way layers are deposited to create parts, in the operating principle and in the materials that can be used. Some methods melt or soften materials to produce the layers, e.g. selective laser melting (SLM), selective laser sintering (SLS) and fused deposition modelling (FDM), while others cure liquid materials, e.g. stereolithography (SLA). Each method has its own advantages and drawbacks, and some companies consequently offer a choice between powder and polymer for the material that the object is built from. The main considerations made for choosing a machine are generally its speed, its cost that of the printed prototype, the cost and range of materials as well as its colour capabilities [8]. Nowadays, there is a significant tendency towards AM of structural, load-bearing structures, by taking advantage of the inherit design freedom of such a process. Those structures need to be
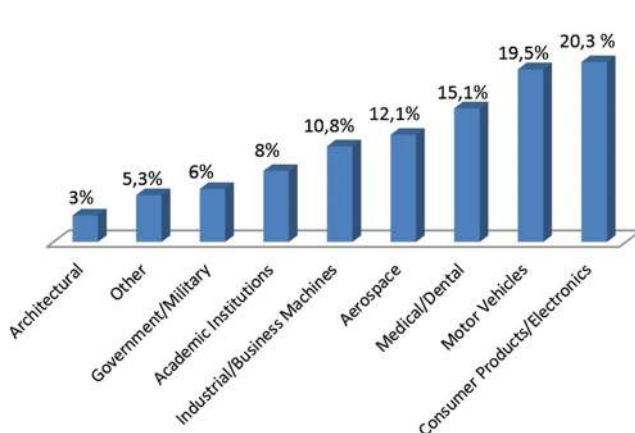

Fig. 2 Breakdown of the percentage of the industrial sectors using AM [6]

built from metal; therefore focus is given to processes, such as SLS/SLM, DMD and EBM for industrial uses.

2.1 Laser-based processes

Laser-based additive manufacturing processes use a laser source of medium to low power in order to melt, solidify or cure the material. The laser-based processes can be distinguished in two sub-categories, depending on the phase change mechanism, namely laser melting and laser polymerization. In the laser melting processes, the material is supplied, in the form of powder, either to a powder bed or via nozzles directly to the processing head. A laser beam is used in order to melt the material, which then cools down and solidifies in order for the part to be produced. In laser polymerization, the material is usually a photosensitive resin, which is being cured upon its exposure to UV radiation, provided by a low-power laser source.

2.1.1 Laser polymerization

All laser polymerization additive manufacturing processes are based on the same material phase change principle; a liquid photosensitive resin that solidifies upon illumination from a (usually a low-power) laser source. Laser polymerization processes are limited in producing polymer parts of relatively low-strength resin, therefore, they are usable in prototyping and non-structural applications rather than in structural parts' production (Fig. 4).

Stereolithography (SLA) Stereolithography is based on the photopolymerization principle of photosensitive monomer resins when exposed to UV radiation. The UV radiation source is a low-power He-Cd or Nd: YVO4 laser (up to 1000 mW in modern machines [10]) that solidifies a thin layer on the surface. An SLA machine mainly consists of a built platform, which is immersed into a bath of liquid resin and a laser source, including the appropriate hardware and software for control. A layer of the part is being scanned on the resin surface by the laser, according to the slice data of the CAD model. Once the contour of the layer has been scanned, the interior is crosshatched and hence solidified; the platform is being submerged into the resin, one layer below. A blade sweeps the surface to ensure flatness and the next layer is built, whilst simultaneously is attached to the previous one [11].

Solid ground curing (SGC) SGC is a photo-polymer-based additive manufacturing technology in which the production of the layer geometry is carried out by means of a high-powered UV lamp or laser source through a mask [12]. SGC was developed and commercialized by Cubital Ltd. in 1986. While the method offers good accuracy and a very high build rate, it

Fig. 3 Rapid prototyping worldwide 2001 [7]

Fig. 3 Rapid prototyping worldwide 2001 [7]
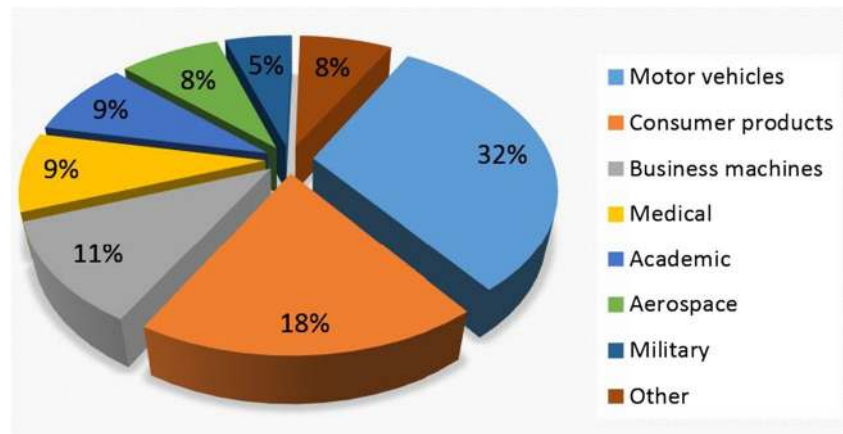
bears high operating and changeover costs due to the system's complexity.

Liquid thermal polymerization (LTP) LTP is a process similar to SLA in the way that the part is built by solidification of successive layers of liquid polymer. However, the polymers used in LTP are thermosetting instead of photopolymers and hence, the solidification is induced by thermal energy rather than light. The thermal nature of the process makes the control of the size of the polymerization zone difficult, due to the dissipation of heat [13], therefore, the parts produced by this method are less accurate. Nevertheless, the process has a relatively high throughput and can be considered in applications where accuracy is not an issue.

Beam interference solidification (BIS) BIS is based on point-by-point solidification of photosensitive polymers at the intersection of two laser beams having different wavelengths. The first laser excites the liquid polymer to the

Fig. 4 Laser polymerization AM process schematic [9]

reversible metastable state, which is subsequently polymerized by the radiations of the second laser. The process is associated with various technical limitations such as insufficient absorption of laser radiation at higher depths, shadowing effects of the already solidified material and diffraction of laser light, leading to difficulties in obtaining the precise intersection of the beams [13].

Holographic interference solidification (HIS) In this process, a holographic image is projected on a liquid photosensitive polymer contained in a vat so as for the entire surface of the polymer to be solidified, instead of point-by-point [13]. In that essence, the process is really similar to that of solid ground curing.

2.1.2 Laser melting

Laser melting additive manufacturing processes use a laser source to selectively melt a material supplied in the form of fine powder. The material then cools down and solidifies to form the final part. Scanning optics is being used to steer the laser beam in the *x-y* plane, while a table moves towards the *z*-direction (Fig. 5).
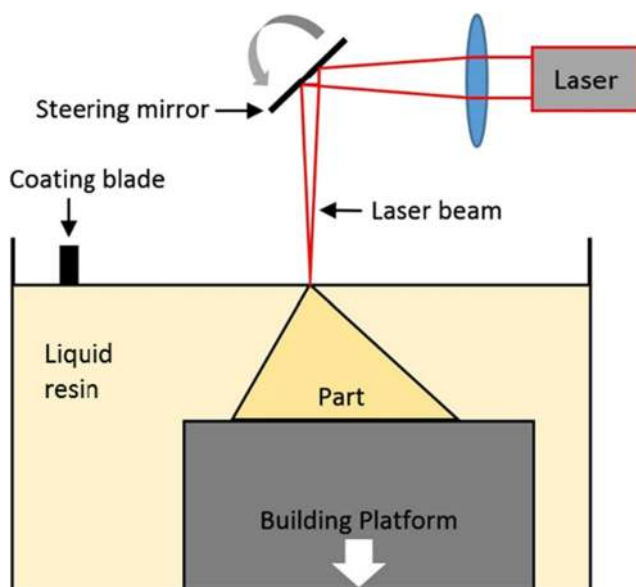
Selective laser sintering (SLS) Selective laser sintering uses a fine powder, which is heated by a laser beam (ranging from 7 W for plastic [14] up to 200 W [15, 16]) in such a way so as to allow the grains to fuse together [17]. Albeit the process is known as sintering, it is not entirely true. Before the powder is sintered by the laser beam, the entire bed is heated just below the melting point of the material in order to minimize thermal distortion and facilitate fusion in the previous layer. After each layer has been built, the bed is lowered and a new powder layer is applied. A rotating roller is then used to spread the powder evenly. The sintered material forms the part, while the unsintered material powder remains in place to support the structure. The unsintered material may be cleaned away and recycled after the build has been completed. Materials, such as
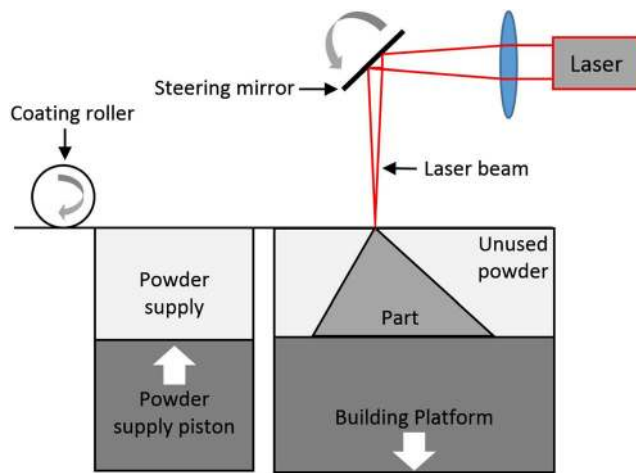
Fig. 5 Laser melting AM process schematic [9]

metal powders, nylon, nylon composites, sand, wax and polycarbonates, can be used [17]. However, the process is still relatively slow (when compared to EBM for metallic structures for instance) and suffers from issues such as non-uniform thermal field distribution, which might lead to thermal distortion and cracks on the product. Despite that, SLS's high degree of accuracy and surface quality renders it one of the most commonly used metal AM processes.

Selective laser melting (SLM) Selective laser melting is a process similar to SLS; the two are instantiations of the same concept but differ in technical details. Instead of sintering, in the SLM process, powder melting occurs in order to form a part. Therefore, laser beam power is usually higher (around 400 W).

Direct metal laser sintering (DMLS) Direct metal laser sintering is another commercial name used for the description of a laser-based additive manufacturing process, similar to SLS/SLM. However, while SLS/SLM is able to process a variety of materials, the DMLS processes metallic powder only. The DMLS has been developed by EOS and it is a trademarked name. The typical laser power of the EOS machines is 200–400 W [18].

Laser engineered net shaping (LENS) Laser engineered net shaping uses a high-power laser to melt metal powder. A specially designed powder delivery nozzle injects the powder stream directly into the focused laser beam, and the laser head and powder nozzle move as an integral unit. Metal powders are delivered and distributed around the circumference of the head either by gravity or by using a pressurized carrier gas. The laser beam creates a small molten pool on the substrate or previously deposited layers. The powder fed into this region is consumed in this puddle, causing its height to grow away from the substrate surface. The x-y table is moved to fabricate each layer of the object. The head is moved up vertically as each

layer is completed. This technique is equivalent to several trademarked techniques, such as DMD, LPD and SLC [18]. Compared to processes that use powder beds, such as SLM, objects created with this technology can be substantially larger, even up to several meters long; however, the accuracy and surface quality are usually lower.

Direct metal deposition (DMD) DMD is an additive manufacturing technique that uses a laser as the power source to sinter or melt powdered material (typically metal), with the laser automatically aiming at points in space, defined by a 3D model, binding the material together to create a solid structure. The operating principle is really close to the SLS/SLM process, albeit lacking in a powder bed; instead powder is fed by a number of nozzles (usually 3) directly to the processing head, similar to that of LENS.

Laser powder deposition (LPD) In this layered manufacturing process, a powder/air stream is injected directly into the laser beam focus point on the substrate [19]. Variants of this process are LENS, SLC, SDM and DMD [20].

Selective laser cladding (SLC) Selective laser cladding is another commercial material processing technique that uses the laser as a heating source to melt metal powder to be deposited on a substrate. This technique is being applied, as a rapid manufacturing (RM) process, to generate a point-by-point and a layer-by-layer part. It has been introduced as a means of creating functional metal parts with near-net shape geometries and has a significant advantage over the traditional RP techniques. This is due to the direct fabrication of a near-net shape part compared to the two-step process, involving an intermediate step of mould preparation in conventional RP techniques [21].

2.2 Extrusion processes

The material extrusion processes are thermal and use a heated extrusion nozzle in order to soften or melt material, usually plastic, provided in the form of wire. After being melted, the material passes through an extrusion nozzle that deposits the material, which then cools off in order to solidify and form the final part geometry (Fig. 6).

2.2.1 Fused deposition modelling (FDM)

The FDM technique uses a movable head, which deposits a thread of molten thermoplastic material onto a substrate. The material is heated up to 1 °C above its melting point, so that it solidifies right after extrusion and subsequently welds to the previous layers. The FDM system head usually includes two nozzles, one for the part material and one for the support material. The system's advantage is that it can be viewed as

Fig. 6 Extrusion AM process principle and schematic [14]
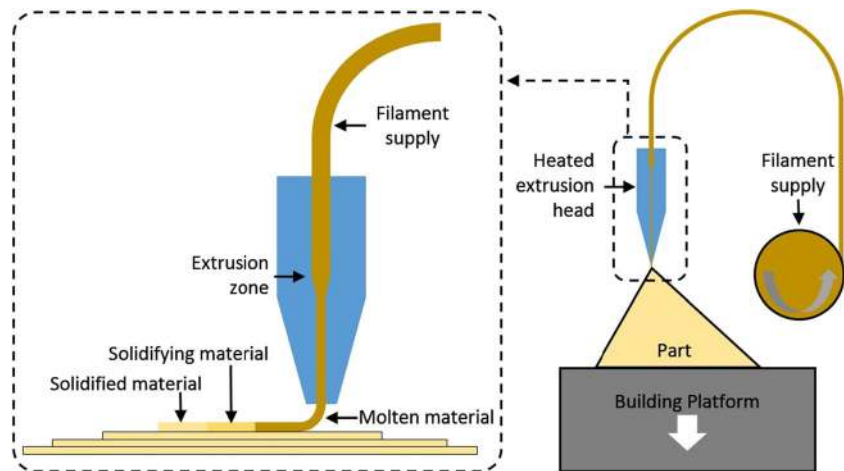
a desktop prototyping facility, since it uses cheap, non-toxic, odourless materials, in a variety of colours and types, such as acrylonitrile butadiene styrene (ABS), medical ABS, PLA, investment casting wax and elastomers [17]. The simplicity of the FDM process, the relatively cheap equipment and the raw materials render its use ideal by hobbyists as well as the production of low-cost plastic parts. However, accuracy and surface quality are relatively poor when compared to those of powder-based plastic AM processes.

2.2.2 Robocasting

Robocasting is a freeform fabrication technique that is based on layer-wise deposition of highly loaded colloidal slurries for dense ceramics and composites. The process is essentially binderless with less than 1 % organics and the parts can be fabricated, dried and completely sintered in less than 24 h [22].

2.3 Material jetting

The material jetting processes use thin nozzles in order to "spray", in a controlled manner, either molten material or more usually a binder (adhesive) in order to bind the powder in a solid object. The process operating principle is much like all the laser-melting processes, albeit no phase change occurs; instead, the binder holds the powder particles together (Fig. 7).

2.3.1 Three-dimensional printing (3DP)

3DP is a layered manufacturing process, where parts are created inside a piston, containing a powder bed. In more detail, the piston is gradually dropped and a new layer of powder is spread across the top. The part is formed by "inkjet printing" the binder into the powder [23].

2.3.2 Inkjet printing (IJP)

IJP is a type of computer printing that creates a digital image by propelling droplets of ink onto paper, plastic or other substrates. Inkjet printers are the most commonly used types of printers and range from small inexpensive consumer models to very large professional machines that can cost tens of thousands of dollars or more [23].

2.3.3 Multijet modelling (MJM)

The principle underlying MJM is the layering principle, used in most other RP systems. The MJM builds models using a technique akin to inkjet printing applied in three dimensions. The MJM head moves in the x-y plane, depositing special thermo-polymer material only where required, building a single layer of the model. A UV lamp flashes through each pass to cure the thermo-polymer deposited. When the layer is complete, the platform is distanced from the head (z-axis) and the head begins building the next layer [13].
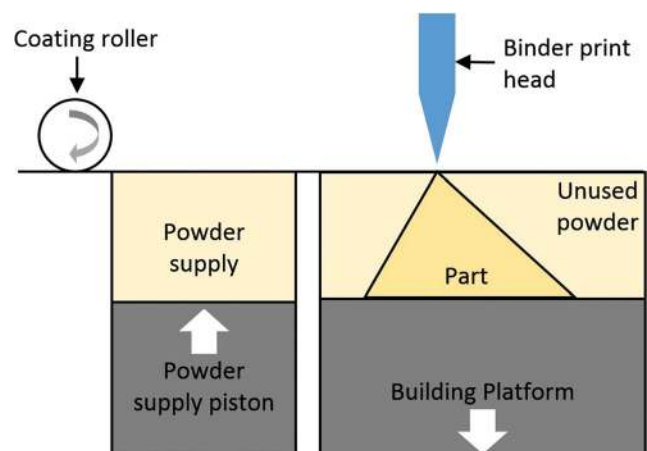
Fig. 7 Material jetting AM process principle and schematic [9]

2.3.4 Ballistic particle manufacturing (BPM)

The BPM process involves a stream of molten droplets ejected from piezoelectric inkjet printing nozzles to be deposited on the target substrate. The process still uses the 3D data of the solid model to position the stream of material on the substrate. Since the process is based on the material's melting, it is particularly suited for the materials, namely thermoplastics and metals that easily melt and solidify [13].

2.3.5 Thermojet

Thermojet is a process similar to multijet modelling. The system generates wax-like plastics models, albeit with less accuracy than SLA. The machine uses a wide area head with multiple spray nozzles. These jetting heads spray tiny droplets of melted liquid material which cool and harden on impact to form the solid object. This process is commonly used for the creation of casting patterns in the jewelry industry and other precision casting applications.

2.4 Adhesive

Adhesive-based processes are of limited use nowadays. The operating principle involves (usually a laser) a cutter, which cuts a thin film of paper or plastic in the desired outlines. The film is then pressed down onto the previous one by a heated compactor, thus activating a heat curing adhesive present on the downwards face of the film, in order to be bonded to the substrate (Fig. 8).
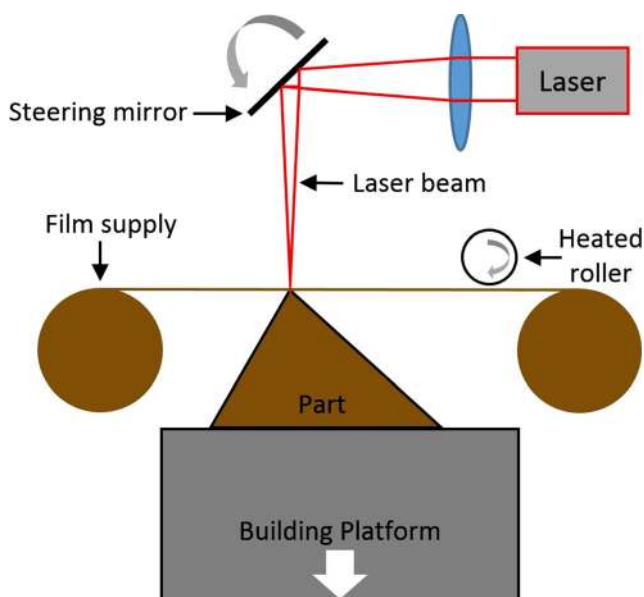
2.4.1 Laminated object manufacturing (LOM)

The material used in LOM is a special kind of paper, having a heat-sensitive adhesive applied to one of its sides. The paper is supplied from a roll and is bonded to the previous layer with the use of a heated roller, which activates the paper's adhesive. The contour of the layer is cut by a CO_2 laser, carefully modulated to penetrate into a depth of exactly one layer (paper) thickness. Surplus waste material is trimmed to rectangles to facilitate its removal but remains in place during build-in order to be used as support. The sheet of material used is wider than the building area, so that, when the part layer has been cut, the edges of the sheet remain intact in order to be pulled by a take-up roll and thus to continuously provide material to the next layer [17].

2.4.2 Solid foil polymerization (SFP)

The process is based on complete polymerization of semi-polymerized plastic foils on exposure to suitable light source. The semi-polymerized foil is first stacked on the previously solidified part and then illuminated such that bonding is achieved after complete polymerization. The excess foil that is not illuminated can be removed by being dissolved into suitable solvent, leaving behind the desired part [13].

2.5 Electron beam

Electron beam processes are identical to the laser-melting processes but instead of a laser beam, an electron beam is used as an energy source in order to melt or sinter the material (Fig. 9).
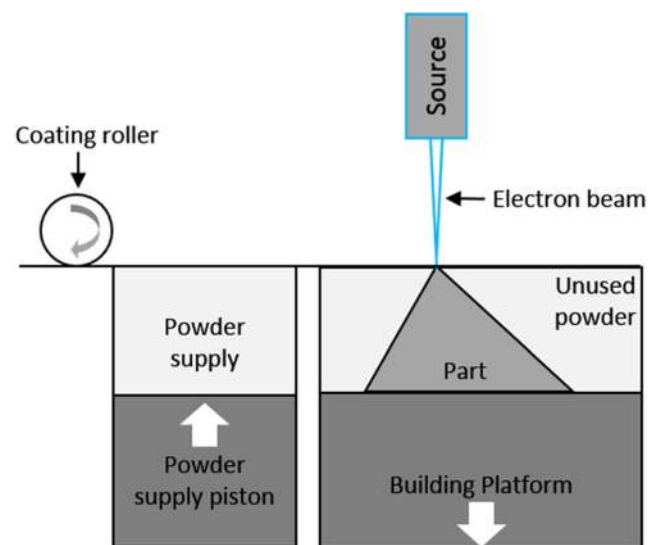

Fig. 8 Adhesive AM process schematic [9]

Fig. 9 Electron beam AM process schematic

2.5.1 Electron beam manufacturing (EBM)

EBM is a relatively new but rapidly growing process similar to SLS, albeit suitable for building metallic parts only. Powder is melted by an electron beam powered by a high voltage, typically 30–60 KV. The process takes place in a high vacuum chamber to avoid oxidation issues. EBM can also process a high variety of pre-alloyed metals [24]. When compared to SLS, EBM can offer much higher throughput and more uniform thermal field distribution; however, accuracy and surface quality are lower.

2.6 Comparative table

The categorization of AM processes can be summarized in Table 1.

3 Modelling approaches

The AM processes are hampered mainly due to their low productivity, relatively poor surface quality and dimensional stability as well as uncertainty regarding the mechanical properties of the products. Therefore, those manufacturing attributes should be optimized in order for AM to get established in production. For the optimization of any manufacturing process, a deep knowledge of the process itself is required. This knowledge could be gained, either by experimentation or by analysing the physical mechanisms of the process. A model is the abstract representation of a process that establishes a relation between input and output quantities. The real system is simulated by the models that aim to predict its performance.

Models met in literature can be divided into three major categories, namely analytical, numerical and empirical ones, depending on the development approach. The analytical models are the output of the process's mathematical analysis, taking into consideration the physical laws and the relevant physical processes. The main advantage of such models is that the derived results can be easily transferred to other pertinent processes. The limits of the analytical modelling are determined by the underlying assumptions. The empirical models, on the other hand, are the outcome of a number of experiments, whose results are evaluated; one model type is chosen, the coefficients are determined, and then the empirical model can be verified by further tests. The quality of the models' results is limited in the special conditions of the specific process. Their major advantage, compared with that of the analytical models, is that they require minimum effort. Numerical models are in between, in essence, stem from the physics of the process, but a numerical step-by-step method is employed over time in order for useful results to be produced. Following is a list of authors who have presented modelling attempts in AM.

Table 2 presents a categorization of those attempts, based on the method (analytical, numerical and statistical/empirical) used to model the desired attribute. Moreover, Table 3, at the end of Section 3, presents modelling approaches categorized on the basis of the modelled attribute, both for the AM products (accuracy, roughness, integrity etc.) as well as for the process (phase change, heat transfer etc.)

3.1 Laser-based processes

In laser-based processes, the most usual modelled aspects are the interaction between the laser beam and the material and the associated phase changes, either from liquid to solid (photopolymerization) or from solid to liquid (melting).

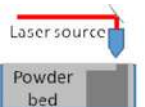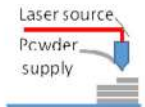**Table 1** Additive manufacturing process categorization
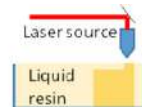
	Additive Manufacturing (AM) Processes							
Process	**Laser Based AM Processes**			**Extrusion Thermal**	**Material Jetting**	**Material Adhesion**	**Electron Beam**
	Laser Melting		*Laser Polymerization*				
Process Schematic	Laser source / Powder bed	Laser source / Powder supply	Laser source / Liquid resin	Material melt in nozzle	Material jetting	Laser cutting / Compactor	Electron beam / Powder bed
Name / Material	SLS	DMD	SLA	FDM	3DP	LOM	EBM
	SLM	LENS	SGC	Robocasting	IJP	SFP	
	DMLS	SLC	LTP		MJM		
		LPD	BIS		BPM		
			HIS		Thermojet		

Bulk Material Type	Powder	Liquid	Solid

Table 2 AM modelling approaches categorized according to modelling method

Process		Modelling method		
Type	Name	Analytical	Numerical	Empirical
Laser-based (polymerization)	SLA	[25–33]	[34, 35]	[36–49]
Laser-based (melting)	SLS	[50]	[51–58]	[59]
	SLM	[60, 61]	[51, 52, 60, 62, 63]	
	DMD	[56]		
	LPD		[64, 65]	
	SLC		[55, 66, 67]	
Extrusion (thermal)	FDM	[57, 68–72]	[68, 72–78]	[58, 79, 80]
Material jetting	3DP	[65]	[81, 82]	
Adhesive	LOM			[33]
Electron beam	EBM		[83–87]	

3.1.1 Laser polymerization

Chryssolouris in [88] has used a semi-empirical approach through statistical design to extract a model, regarding the dimensional accuracy of AM parts built via stereolithography; thus identifying the most crucial process parameters that affect accuracy in each direction built. Retraction (the distance of the hatch vector end from the layer border) is not only the dominant parameter in the x-direction but also important to the y-direction accuracy; whereas, in the z-direction, the shrinkage compensation function was found to be the most influential. Zhou et al. [47] as well as others [39, 40] have used a similar, semi-empirical approach by the Taguchi experimental design

techniques and process the results with the response surface methodology and analysis of variance (ANOVA) methods, to investigate into the optimal parameters (including layer thickness, hatch spacing, hatch style, hatch overcure, blade gap, position on the build plane) of the platform of the SLA process. The issue has also been experimentally modelled, by [36–38, 89] having presented experimental studies on the dimensional accuracy of the SLA parts and the associated process parameters. A process planning method was developed by Lynn et al. [41, 42] and was further improved by West et al. [34] in order to develop response surface models for the evaluation of the SLA parts' accuracy. An interesting approach was presented by Cho et al. [48], modelling the SLA process

Table 3 AM modelling approaches categorized according to modelled attribute

Process		Modelled attribute								
Type	Name	Product					Process			
		Surface roughness	Dimensional accuracy	Dimensional stability	Build time	Mechanical properties	Heat transfer	Material deposition/ melt pool	Phase change	Other
Laser-based (polymerization)	SLA	[25, 26, 49]	[34–42, 48, 88, 89]	[27, 43–46, 90]	[30–32, 91]		[25, 29, 30]		[25, 29, 30]	
Laser-based (melting)	SLS			[54, 59]		[53, 92, 93]	[50, 51, 53, 84, 92–94]	[51, 52, 62]		
	SLM	[61]				[63]	[60, 63]	[52, 62]		
	DMD		[56]			[64]		[64]		
	LPD					[64, 65]		[64]		
	SLC					[67]	[66]	[66]	[55]	
Extrusion (thermal)	FDM	[58]		[74]		[77, 80]	[68, 70, 72, 75, 76]	[73]		[57, 68–71, 79]
Material jetting	3DP	[81]						[65, 82]		
Adhesive	LOM	[33]								
Electron beam	EBM					[83]	[83–85]	[86, 87]	[83]	

via a genetic algorithm model in order to determine the optimal process parameters (which include layer thickness, hatch spacing and hatch overcure) that would yield the minimum part build error. Chryssolouris et al. [25] has estimated the average surface roughness of SLA-produced parts as a function of the layer thickness and the angle of the inclined surface (Fig. 10). Modelling was based on simplistic trigonometry assumptions, while the surface roughness could be calculated according to the following equation:

$$R_a = D_p \cdot \ln\left[\sqrt{\frac{2}{\pi}\frac{P_L}{W_0 V_S E_C}}\frac{\sin\theta}{4\tan\theta}\right] - OC\frac{\sin\theta}{4\tan\theta} \quad (1)$$

where:

D_p depth of penetration
P_L laser power
W_0 laser beam spot diameter
V_S laser scanning speed
E_C critical exposure time
OC overcure

Reeves and Cobb in [26] and [49] presented an analytical model for SLA surface roughness that took into consideration the layer profile as well whether the plane was up-facing or down-facing, which was verified with experimental data. Podshivalovab et al. [35] has used a 3D model to verify the dimensional accuracy of scaffold-like structures used in bone replacement via CAD and FEA. Part dimensional stability has been experimentally studied by a number of researchers. Rahmati [43] studied dimensional stability in SLA as a result of resin shrinkage; Wang et al. [44] studied the effect of the post-curing duration, the laser power and the layer pitch on the post-cure shrinkage and empirical relations were established on the basis of the least squares method. The shrinkage strains were investigated by Karalekas and Aggelopoulos [45] based on a simple experimental setup and the elastic lamination theory. Narakahara et al. [46, 90] studied the relationship between the initial linear shrinkage and resin temperature in a minute

volume built by SLA. Flach et al. [27] integrated an analytical resin shrinkage model into the general SLA process model developed in [28], to have a theoretic prediction of the dimensional stability due to resin shrinkage, concluding that faster shrinking resins should result in lower overall shrinkage values. It has been found that the overall linear shrinkage, due to cure for a line of plastic, was estimated to have been given by the equation:

$$F_C = 1/L \int_0^L f_r(Y) dy \quad (2)$$

where:

$f_r(y)$ residual fractional linear shrinkage at position y
F_C overall fractional linear shrinkage due to cure
L length of strand of plastic (cm)
t time (sec)
t_s time for laser to scan from position y to L (sec)

Chryssolouris [25], Jelley [29] and Jacobs [30] investigated the polymerization process that occurs during SLA manufacturing, based on the modelling of the laser source, the modelling of the photo-initiated free radical polymerization and the modelling of the heat transfer involved in the process. A few have dealt with modelling the build time in the SLA process. Chen [31], Giannatsis [91] and Kechagias [32] have calculated the process time analytically. Kechagias [32] has presented a method where the total distance travelled by the laser beam is directly calculated from the part geometry (STL file). The time required for each layer to be produced is then calculated analytically on the basis of the laser velocity, keeping in mind whether the laser is performing border drawing, hatching or filling. Furthermore, the time required for all the auxiliary steps is estimated. Contouring and hatching velocities were calculated by:

$$Cv(i) = \sqrt{\frac{2}{\pi}\frac{P_L}{W_0 E_C e^{\left(Cd(i)/Dp\right)}}}, \quad (3)$$

$$Hv(i) = \frac{mP_L}{hs E_C e^{\left(Cd(i)/Dp\right)}} \quad (4)$$

where:

P_L laser power
W_0 laser beam half width
Cd curing depth
hs hatching space (distance between neighbour scanning vectors)
m number of times the slice area is hatched
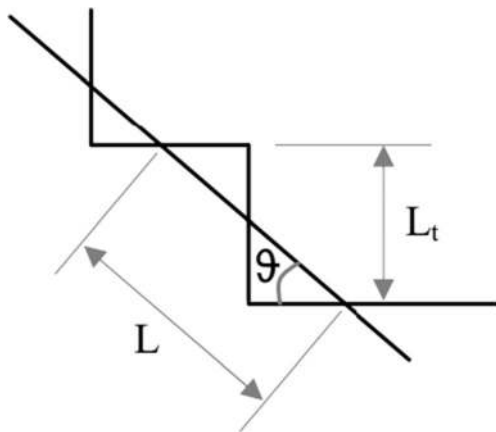E_c critical energy
Dp penetration depth

Fig. 10 Trigonometry used by Chryssolouris [25]

It has been found that the hatching time, calculated as the ration between the total hatching length $Hl(i)$ and the hatching velocity $Hv(i)$ deviates from the actual one, due to delays occurring during hatching; further experimental study of the hatching procedure has led to the following equation, the accuracy of which was found to be within 0.5 %.

$$\text{THatch} = \frac{Hl(i)}{Hv(i)} + 0.0005\text{NoVectors}$$
$$+ \frac{Hl(i)}{54Hv(i)+6114} - 0.206. \quad (5)$$

Jacobs [30] assumed that the laser presents a Gaussian distribution and the absorption of the laser radiation within the resin follows the Beer-Lambert Law. Based on these assumptions, he calculated the maximum depth of the cured line. Based on the relation among the maximum exposure, the laser power, the half beam width and the scanning speed, required for their solidification to a specific cure depth, were calculated:

$$V_s = \sqrt{\frac{2}{\pi}} \left[\frac{P_L}{W_0 E_C} \right] \exp\left(-\frac{C_d^s}{D_p} \right) \quad (6)$$

Chen et al. [31], based on Jacobs' work [30], developed an analytical model for predicting total build time, by incorporating a correction factor based on experimental work. The model has been found to be in good correlation with experimental data for a number of different parts.

3.1.2 Laser melting

Wang and Kruth [50] modelled the laser beam scanning and the energy absorption, taking place in an SLS machine, by using the analytical ray-tracing model which allowed the calculation of the sintering zone dimensions (width and thickness). The energy necessary to fuse a certain powder particle can be calculated according to the following equation:

$$E_m = \left(c_p \times \Delta T + c_l \right) \times \rho \times V \quad (7)$$

where:

c_p specific heat (*KJ/KgK*)
ΔT temperature rise required for melting (*K*)
c_l latent melt energy (*KJ/Kg*)
ρ density (*kg/mm³*)
V volume of the (spherical) particle (*mm³*)

A simple comparison of the absorbed energy E_i to E_m will determine whether any particle absorbs enough energy to melt or not. The sintering zone dimension is evaluated from the most side-wise molten particles.

Chen and Zhang [51] investigated the parameters affecting the sintering depth and shape of the liquid pool by formulating a temperature-transforming 2D numerical model. This model converts the enthalpy-based energy equation into a nonlinear equation with temperature being the only dependent variable. Vasinonta et al. [64] have developed two process maps for laser-based solid freeform fabrication processes, through the investigation of the melt pool size and the residual stresses developed via finite element thermomechanical models. Michaleris [60] investigated two finite element techniques for modelling metal deposition and transient conducting heat transfer in SLM. Particularly, quiet and inactive element activation is probed. In the quiet case study, the elements are manipulated through their properties in order to be neutral. In the inactive case study, the elements are not included in the analysis until the related material has been added. Analytical equations have been used for the formulation of transient conductive heat transfer. The evaluation has been performed by the use of 1D and 3D FEA models. Zhiqiang [62] investigates the topic of fusion-based additive manufacturing of titanium through the use of mathematical and numerical modelling in order to model the melt pool. The numerical model was correlated with experimental measurements. Melt pool monitoring was an attribute also investigated into by Hu and Kovacevic in [52] using a 3D numerical model. Matsumoto et al. [63] proposed a simulation method about a single layer deposition of the SLM process. The stress and temperature within the solid layer have been calculated with the heat conduction and linear finite elements. Kolossov et al. [94] modelled the heat transfer and thermal field using a nonlinear 3D model, which took into consideration the thermal characteristics of bulk material, such as thermal conductivity and heat capacity and the thermal history of the material in each step. Dong et al. [53] created a 3D FEA model to predict statistically the temperature and density distribution in the SLS of polycarbonate. The parameters analysed include the laser beam velocity, laser power and laser diameter, and the results have been verified against experimental values found on related literature. A similar approach was followed by Liu [92], developing a micro-scale 3D FEM in order to investigate the characteristics of the temperature distribution within the powder bed. Giovanni et al. [61] investigated the surface roughness and morphology in SLM parts. A mathematical model is introduced for the prediction of surface roughness. Both the stair step effect and the increasing presence of particles on the top surface are considered key contributing factors to the surface morphology. In Khairallah [93], a mesoscopic 3D model has been introduced to simulate the SLM processes by using the commercial code ALE3Dmulti-physics. The simulation includes the substrate, the random particle melding and re-solidification either into a continuous or a discontinuous track. The model is taking into consideration the thermal diffusion to hydrodynamics, the temperature-dependent material properties, the surface tension and the random particle distribution.

Various researchers have investigated shrinkage in SLS. Chen and Zhang [54] created a partial shrinkage model of

two component metal powder mixture with different melting points, in order to investigate the effects of volume fraction of the gas in the liquid or sintered regions on the shape and size of the heat-affected zone. Furthermore, Raghunath and Pandey [59] utilized the Taguchi method for the determination of the influence of the SLS process parameters to shrinkage, as well as to define the optimum shrinkage conditions.

LPD, DMD and SLC are variations of the same process, where a powder is injected into a laser beam and melted simultaneously with a thin layer of the substrate to form a continuous track of material. Costa et al. [95] developed a thermo-kinetic FE model of multilayer LPD for the investigation of the microstructural transformations and hardness variations that occur during the deposition of steel parts for the calculation of the final hardness distribution in the part. The results obtained were in agreement with published experimental observation. Gockel et al. [83] have developed an FE model capable of simulating the material solidification of Ti64 in an electron beam wire feed AM process resulting in the prediction of the material microstructure and properties. A similar model of the LPD of titanium was developed by Crespo et al. [66] in order to study the influence of the deposition path geometry on the melt pool stability as well as to estimate the adjustments of the deposition parameters, necessary to avoid hot spots. The same thermo-kinetic model has been used in order for the hardness distribution of the SLC process to be predicted [67]. Toyserkani et al. [55] investigated the effects of laser pulse shaping on the SLC process with a 3D FE model. In Muller's work [56], an analytical model of the direct LPD process has been developed, for functionally graded materials (FGM). Particularly, this study focuses on the operation of a powder distribution system. The model scope is to be utilized in order for manufacturing strategies, in the production of parts, to be compared with complex material distribution.

3.2 Extrusion processes

FDM is a process modelled for various attributes. Zhang and Chou [73] developed a 3D FEA model to simulate the FDM process melt pool. The same model was used and enhanced by Zhang in [74] for the simulation of the residual stresses in order for part distortion to be evaluated. Prototype parts were built and used to validating the simulated results. Bellini et al. [68] and Venkataraman et al. [69] have analytically modelled the material flow on the extrusion nozzle. Venkataraman et al. [69] investigated the material buckling in the liquefier using Euler's analysis for buckling and a capillary rheometer. The pressure drop (ΔP) in a capillary rheometer required that a non-Newtonian fluid be driven through a tube of length l and radius r is:

$$\Delta P = \frac{8\eta_\alpha Q l}{\pi r^4} \qquad (8)$$

where:

n_a apparent viscosity determined using a capillary rheometer

Q volumetric flow rate

It was calculated that the filament material would buckle if:

$$E/\eta_\alpha < \frac{8Ql(L/R)^2}{\pi^3 r^4 k} \qquad (9)$$

where:

L/R slenderness ratio of the filament

k scaling factor (experimentally determined)

Yardimici [70] and Agarwala [71] have studied the issue of filament buckling in a liquefier entry by theoretical means. An experimental investigation into the same phenomenon was conducted by Venkataraman [79]. Heat transfer to the built material inside the liquefier was theoretically studied by [68, 70, 72], while a number of authors dealt numerically with the same issue [68, 72, 75, 76].

Ramanath [72] having used Bellini's previous work [68] has mathematically modelled the pressure drop during the extrusion of PCL.

Using the law of non-Newtonian polymer melt flow $\gamma = \varphi \tau^m$, the pressure drops for each of the five zones were derived, by considering Bellini's work [68].

$$\Delta P_1 = 2L_1 \left(\frac{V}{\phi}\right)^{\frac{1}{m}} \left(\frac{m+3}{r_1^{m+1}}\right)^{\frac{1}{m}} \exp\left[\alpha\left(\frac{1}{T-T_0} - \frac{1}{T_\alpha - T_0}\right)\right] \qquad (10)$$

$$\Delta P_2 = 2L_2 \left(\frac{V}{\phi}\right)^{\frac{1}{m}} \left(\frac{m+3}{r_1^{m+1}}\right)^{\frac{1}{m}} \exp\left[\alpha\left(\frac{1}{T-T_0} - \frac{1}{T_\alpha - T_0}\right)\right] \qquad (11)$$

$$\Delta P_3 = 2L_3 \left(\frac{V}{\phi}\right)^{\frac{1}{m}} \left(\frac{m+3}{r_1^{m+1}}\right)^{\frac{1}{m}} \exp\left[\alpha\left(\frac{1}{T-T_0} - \frac{1}{T_\alpha - T_0}\right)\right] \qquad (12)$$

$$\Delta P_4 = \frac{2m}{3\tan\left(\frac{\alpha}{2}\right)} \left(\frac{1}{r_2^{\frac{3}{m}}} - \frac{1}{r_1^{\frac{3}{m}}}\right) \left(\frac{V}{\phi}\right)^{\frac{1}{m}} \left[r_1^2 2^{m+3}(m+3)\right]^{\frac{1}{m}} \exp\left[\alpha\left(\frac{1}{T-T_0} - \frac{1}{T_\alpha - T_0}\right)\right] \qquad (13)$$

$$\Delta P_5 = 2L_5 \left(\frac{V}{\phi}\right)^{\frac{1}{m}} \left[\frac{r_1^2(m+3)}{r_2^{m+3}}\right]^{\frac{1}{m}} \exp\left[\alpha\left(\frac{1}{T-T_0} - \frac{1}{T_\alpha - T_0}\right)\right] \qquad (14)$$

$$\Delta P = \Delta P_1 + \Delta P_2 + \Delta P_3 + \Delta P_4 + \Delta P_5 \qquad (15)$$

where:

$L_1 - L_3$ and L length of respective zones

$$L_2 = \left(\pi\left(R_2 + d_1/2\right)\right)/2$$

R_2 radius of the channel at zone 2
r_1 radius of the cylindrical area of the melt flow channel
r_2 the exit radius
a nozzle angle
V filament velocity at the entry
u fluidity
m flow exponent
T working temperature
Ta the temperature at which m and u are calculated
To the absolute temperature

The model's results were verified with those having derived from the use of an FE model in ANSYS.

Crockett has investigated the deposition and liquid-to-solid transition phase of the FDM process, by developing an analytical model for bead spreading [57]. Sood et al. [80] have developed a semi-empirical methodology using neural network algorithms to develop a model that would predict the compressive strength of FDM built parts. Martinez et al. [77] have used a methodology usually applied to fibrous composite materials for the characterization of parts built by FDM using FEA. Anitha et al. [58] focused on optimizing the FDM process surface quality. Taking into consideration the Taguchi's analysis, three variables have been investigated into, those of the road width, the build layer thickness and the speed of deposition. In addition, analysis of variance (ANOVA) has been performed with the same parameters. Mostafa et al. [78] have performed both 2D and 3D numerical analysis on flow behaviour of ABS-iron composite in FDM, through the ANSYS FLOTRAN and the CFX finite element packages.

Key flow parameters, namely pressure, velocity and temperature, have been investigated into.

3.3 Material jetting processes

3DP has also been the subject of various researchers' study. Jee and Sachs [81] proposed a visual simulation technique so as to facilitate the surface texture designs to be produced by 3DP. This technique simulates 3DP by taking into consideration all the necessary geometric attributes of physical phenomena and therefore enables the realization of a manufacturable design with minimum iterations. Sachs and Vezzetti [82] numerically modelled the deposition process of a new 3DP head design in order to ensure a reliable and continuous jet deposition, resulting in an order of magnitude increase in the printing speed. Curodeau [65] modelled the drop merging (the phenomenon where, in a uniformly spaced train of drops, the leading drop is retarded by air drag and tends to merge with the drop behind it) in order to evaluate the number of merged drops for various distances and printing conditions.

3.4 Adhesive processes

Chryssolouris et al. [33] have used a semi-empirical approach, through a statistical design in order to model the surface roughness of the LOM process. The specific model can predict the part's surface roughness for any combination of process variables.
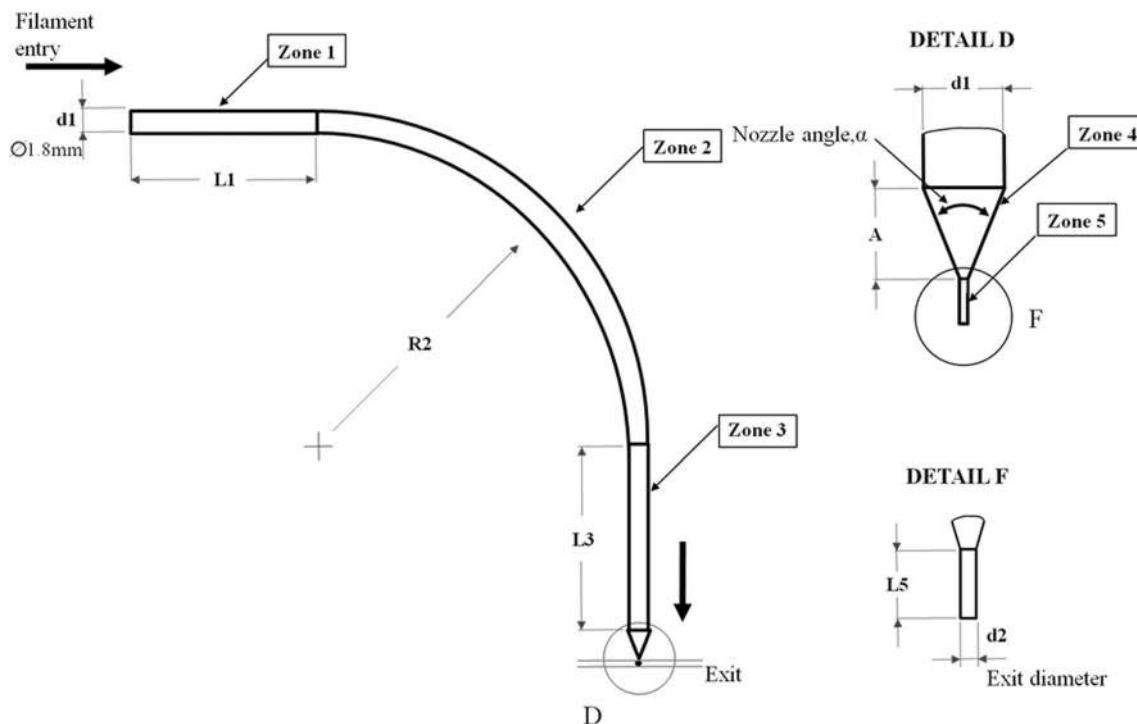

Fig. 11 Sectional view of melt flow channels showing five zones considered by [75]
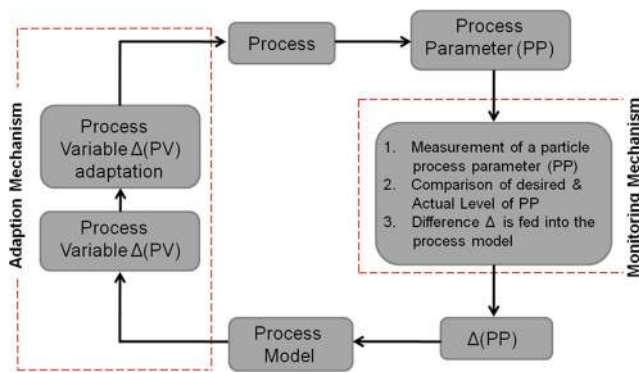
Fig. 12 Process/monitor/control loop [96]

3.5 Electron beam processes

Shen and Chou [84, 85] developed an FE thermal model to investigate the preheating process effect on the EBAM process. Preheating was modelled as a part of the thermal cycle, occurring as initial conditions before the actual electron beam scanning and melting process. Ammer et al. [86, 87] focused on the 3D thermal lattice Boltzmann method for the simulation of the EBAM process, having taken into consideration physical and thermal effects such as melt pool, beam absorption, melting and solidification.

4 Monitoring techniques

For the optimization of a specific AM process, one must measure and quantify the variables of interest. Moreover, the monitoring of process variables enables the verification of process models. In addition, monitoring and control of manufacturing processes is becoming a driver for the manufacturing industries' development and sustainability. Process monitoring is the manipulation of sensor measurements (e.g. force, vision, temperature) in determining the state of the processes. A machine tool operator performs routine monitoring tasks; for example, it visually detects any missing and broken tools as well as the chatter generated from the characteristic sound. Unmanned monitoring algorithms utilize filtered sensor

measurements which, along with operator inputs, determine the process state. The states of complex processes are monitored by a sophisticated signal processing of sensor measurements. The techniques for the monitoring of machining have been traditionally categorized into two methods, namely the direct and indirect.

The techniques of the direct monitoring methods can achieve a high degree of accuracy; however, due to numerous practical limitations, they are characterized as laboratory-oriented techniques. On the other hand, the indirect monitoring methods are less accurate but more suitable for practical applications, at machine shop level. In Fig. 11, the process-monitor-control loop is presented for successful functional systems (Fig. 12).

The main process variables, according to each process are presented in Table 4.

Although there are several additive manufacturing techniques with different working principles and machine setups, it could be identified that the energy providers in all of them are either nozzle based (extrusion processes) or laser based. By further inspection over the machine elements, it could be identified that most of the parts, namely the manufacturing chambers' temperature in SLS, the paper supply in LOM and the height of the building platform in most AM processes, could be monitored with conventional methods such as travel sensors, strain gauges and cameras. On the other hand, the nozzle and laser elements tend to be non-conventional technologies, with variable contingencies. In the next section, monitoring techniques of the basic machine elements will be presented in a generic approach.

4.1 Laser monitoring

Temperature monitoring in laser-based processes is based on optical measurements of the temperature distribution to the sintering/melting zone by using a camera sensor and maximum surface temperature monitoring in the irradiation spot with the use of a high-speed, two-wavelength pyrometer. The brightness and colour temperature measurements are based on Planck's law, which describes the spectral density of electromagnetic

Table 4 Additive manufacturing technique and basic elements

AM process	Monitored attribute							
	Laser power/ distribution	Melt pool temperature	Nozzle temperature	Jet status	Chamber temperature	Chamber vacuum	Platform position	Head position
Laser polymerization processes	X				X	X	X	X
Laser melting processes	X	X			X	X	X	X
Extrusion processes		X	X		X		X	X
Material jetting processes				X	X		X	X
Adhesive processes					X		X	X

radiation intensity emitted from a black body. On brightness or colour temperature determination, the intensity of the thermal radiation from the surface, in the region of laser action, is recorded by a CCD camera or a pyrometer in one or two spectral intervals and is correlated with the ones of the black body simulator, located in the same surface region. The degree of its approximation to the thermodynamic temperature is defined by the accuracy of the material emissivity determination. In creation of the temperature monitoring system, a combination of two types of optical sensors—2D sensor—a digital CCD camera and a single spot sensor pyrometer, based on photodiodes, which integrate thermal radiation emitted by a surface of certain size, are used [97]. This technique could also be used in extrusion, requiring that the nozzle temperature for the material's liquidity control be measured.

4.2 Nozzle monitoring (jetting)

As it has been referred to, in the previous section, one of the dominant elements, in many of the existing additive manufacturing machines, is that of the nozzles. To ensure productivity and reliability as manufacturing tools, the nozzle status needs to be monitored, while the jet failures should be identified. To detect jet failures, the use of piezo self-sensing signals has been proposed. A piezo inkjet head uses a piezo actuator to jet ink droplets. In addition, the piezo actuator can be used as a sensor, by sensing the force that results from the pressure wave of ink inside the inkjet dispenser. The possible causes of jet failures include the inkjet head temperature control failure, the backpressure control failure, wetting on the nozzle surface, the nozzle blockage, etc. For the verification and the detectability of these jet failures, jet images could be acquired for comparison with self-sensing signals [98].

4.3 Mechanical parts: rollers—building platforms—material supplier

The mechanical parts' motion is usually accompanied by monitoring the applied torque or force, with the use of strain gauges or by monitoring the back EMF of the actuator. Furthermore, for the machine's general function, the optical data could be harvested with the use of photo and video recording devices.

5 Conclusions

In the present paper, a review of all AM techniques has been conducted, followed by a review and assessment of modelling approaches. The AM techniques have been categorized based on their operating principle rather than on the materials used, albeit this has also been kept in mind. The categorization was made in a way that it respected the underlying physics behind the material phase change. Subsequently, modelling processes in the field of additive manufacturing were presented and categorized, based not only on the operating principle but also on the modelled process attribute and the modelling methodology.

The most commonly modelled AM process is that of the SLA, followed by the SLS/SLM and FDM. Most authors deal with modelling dimensional accuracy/stability, while quite a few others deal with predicting the mechanical properties of the finished product as well as the total build time.

The most utilized approach to the issue of dimensional accuracy is by empirical models, via statistical methods (ANOVA etc.). Mechanical properties and dimensional stability modelling are usually made by numerical heat transfer models, studying mainly the melt pool and the material phase change, while build time has been investigated both analytically and numerically.

However, most studies present either a theoretical approach with little to no verification compared to that of real-life results, or semi-empirical approaches that may correlate well with specific experiments, but their results are not directly transferrable and expandable to other machines, requiring further experimentation. The AM processes could significantly benefit from accurate, verified models, aided by the use of machine-integrated monitoring systems in order to be able to back up the models with real, measured data. Given the turn of industry to metal AM, the models of laser-based AM and EBM metals are of utmost relevance, especially in the thermal field, dimensional stability and residual stresses, since these factors significantly affect the quality and safety of the final product.

References

1. ASTM Standard. Standard terminology for additive manufacturing technologies, vol. 10.04
2. Gartner AM report. Information on http://www.gartner.com/ document/2598122 Accessed 16 June 2014
3. AM Platform: Additive Manufacturing Strategic Research Agenda: Release 2014. Available online http://www.rm-platform.com/ linkdoc/AM%20SRA%20-%20February%202014.pdf Access 5 Mar 2015
4. Wohlers TT (2014) Wohlers report 2014: additive manufacturing and 3D printing state of the industry: annual worldwide progress report. Fort Collins, Wohlers Associates
5. Wohlers TT (2013) Wohlers report 2013: additive manufacturing and 3D printing state of the industry: annual worldwide progress report. Fort Collins, Wohlers Associates

6. Wohlers TT (2012) Wohlers report 2012: additive manufacturing and 3D printing state of the industry: annual worldwide progress report. Fort Collins, Wohlers Associates

7. Kruth JP, Levy G, Klocke F, Childs THC (2007) Consolidation phenomena in laser and powder-bed based layered manufacturing. CIRP Ann Manuf Technol 56(2):730–759

8. Pham DT, Dimov SS (2001) Rapid manufacturing, Springer-Verlag, p 6

9. Woesz A (2010) Rapid prototyping to produce porous scaffolds with controlled architecture for possible use in bone tissue engineering. Virtual Prototyp Bio Manuf Med Appl 171–206

10. 3DSystems SLA production series brochure, Information on http://www.3dsystems.com/sites/www.3dsystems.com/files/sla-series-0514-usen-web.pdf Accessed 3 May 2015

11. Salonitis K, Tsoukantas G, Stavropoulos P, Stournaras A (2003) A critical review of stereolithography process modeling, (VRAP 03), 3rd International Conference on Advanced Research in Virtual and Rapid Prototyping, Leiria, pp 377–384

12. Gebhardt IA (2003) Rapid prototyping: industrial rapid prototyping system: prototyper: solid ground curing, Cubital, pp. 105–109

13. Dahotre NB, Harimkar S (2008) Laser fabrication and machining of materials, Springer

14. Kruth JP (1991) Material incress manufacturing by rapid prototyping techniques. Keynote Paper, CIRP Ann - Manuf Technol 40(2):603–614

15. Castoro M (2013) Impact of laser power and build orientation on the mechanical properties of selectively laser sintered parts. Proceedings of The National Conference on Undergraduate Research (NCUR). University of Wisconsin La Crosse, WI

16. 3DSystems SLS production series brochure, Information on http://www.3dsystems.com/sites/www.3dsystems.com/files/sls-series-0214-usen-web_1.pdf Accessed 23 Apr 2015

17. Chryssolouris G (2005) Manufacturing systems: theory and practice, 2nd edn. Springer, New York

18. Khaing MW, Fuh JYH, Lu L (2001) Direct metal laser sintering for rapid tooling: processing and characterization of EOS parts. J Mater Process Technol 113:269–272

19. Vilar R (2014) Laser powder deposition. comprehensive materials processing 2014. Adv Addit Manuf Tooling 10:163–216

20. Ready for Printing - 3D Printing at Siemens video. Information on http://youtu.be/VyEgbyNg0Q8?t=3m46s Accessed 16 June 2014

21. Liu J, Li L (2004) In-time motion adjustment in laser cladding manufacturing process for improving dimensional accuracy and surface finish of the formed part. Optics Laser Technol 36:477–483

22. Cesarano J, King BH, Denham HB (1998) Recent developments in robocasting of ceramics and multimaterial deposition, Proceedings of the 9th Solid Feeeform Fabricatuion Symposium, pp 697–704

23. Pandremenos J, Paralikas J, Chryssolouris G, Dybala B, Gunnink JW (2008) RM product development: design principles, simulation and tool. International Conference on Additive Technologies, Ptuj

24. Wong KV, Hernandez A (2012) A review of additive manufacturing. Int Sch Res Netw Mech Eng 2012:1–10

25. Chryssolouris G et al Deliverable D.2.2.2—development of an analytical model. Research project "Flexible Assembly and Manufacturing Engineering (FLAME)" funded by Greek Secretariat for Research and Technology (GSRT)

26. Reeves PE, Cobb RC (1997) Surface roughness investigation of Stereolithography ACES components. Proceedings of the Second National Conference on Rapid Prototyping and Tooling Research, pp 17–26

27. Flach L, Chartoff RP (1994) A simple polymer shrinkage model applied to stereolithography. Proceedings of the Solid Freeform Fabrication Symposium, pp 225–233

28. Flach L, Chartoff RP (1992) Stereolithography process modelling – a step towards intelligent process control. Proceedings of the Third International Conference on Rapid Prototyping, pp 141–147

29. Jelley C, Thompson CP The development and application of a Stereolithography build simulator. Proceedings of the First National Conference on RP & Tooling Research

30. Jacobs PF (1992) Fundamentals of stereolithography. Proceedings of the Solid Freeform Fabrication Symposium, pp 196–211

31. Chen C, Sullivan P (1996) Predicting total build-time and the resultant cure depth of the 3D stereolithography process. Rapid Prototyp J 2(4):27–40

32. Kechagias J, Anagnostopoulos V, Zervos S, Chryssolouris G (1997) Estimation of build times in rapid prototyping processes. 6th European Conference on Rapid Prototyping & Manufacturing, Nottingham, pp 137–148

33. Chryssolouris G, Kechagias JD, Kotselis JL, Mourtzis DA, Zannis SG Surface roughness modelling of the Helisys laminated object manufacturing (LOM) Process. 8th European Conference on Rapid Prototyping and Manufacturing, Nottingham, pp 141–152

34. West AP, Sambu SP, Rosen DW (2001) A process planning method for improving build performance in stereolithography. J Comput-Aided Des 33:65–79

35. Podshivalovab L, Gomesc CM, Zoccac A, Guensterc J, Yosephb PB, Fischerb A (2013) Design, analysis and additive manufacturing of porous structures for biocompatible micro-scale scaffolds. Procedia CIRP 5:247–252

36. Schaub DA, Chu K, Montgomery DC (1997) Optimizing stereolithography throughput. J Manuf Syst 16(4):290–303

37. Lan PT, Chou SY, Chen LL, Gemmill D (1997) Determining fabrication orientations for rapid prototyping with stereolithography apparatus. J Comput-Aided Des 29(1):53–62

38. Pang TH (1995) Accuracy of stereolithography parts: mechanism and models of distortion for a letter-H diagnostic part. Proceedings of the Solid Free Form Fabrication Symposium, pp 170–180

39. Onuh SO, Hon KKB (1998) Optimizing build parameters for improved surface finish in stereolithography. J Mach Tools Manuf 38(4):329–392

40. CarosiA, Pocci D, Luluiano L, Settimeri L (1996) Investigation on stereolithography accuracy on both solid and QuickCast parts. Proceedings of the 5th European Conference on Rapid Prototyping and Manufacturing

41. Lynn CM, West A, Rosen DW (1998) A process planning method and data format for achieving tolerances in stereolithography. Proceedings of Solid Freeform Fabrication Symposium

42. Lynn CC, Rosen DW (2000) Usage of accuracy models in stereolithography process planning. Rapid Prototyp J 6(2):77–86

43. Rahmati S, Dickens PM (1995) Stereolithography process improvement. Proceedings of the First National Conference on Rapid Prototyping and Tooling Research, pp 111–126

44. Wang WL, Cheah CM, Fuh JYH, Lu L (1996) Influence of process parameters on stereolithography part shrinkage. J Mater Des 17: 205–213

45. Karalekas D, Aggelopoulos A (2003) Study of shrinkage strains in a stereolithography cured acrylic photopolymer resin. J Mater Process Technol 6590:1–5

46. Narahara H, Tamaka F, Kishimani T, Igarashi S, Saito K (1999) Reaction heat effects on initial linear shrinkage and deformation in stereolithography. Rapid Prototyp J 5(3):120–128

47. Zhou JG, Herscovici D, Chen CC (2000) Parametric process optimization to improve the accuracy of rapid prototyped stereolithography parts. J Mach Tools Manuf 40:363–379

48. Cho HS, Park WS, Choi BW, Leu MC (2000) Determining optimal parameters for stereolithography process via genetic algorithm. J Manuf Syst 19(1):18–27

49. Reeves PE, Cobb RC (1997) Reducing the surface deviation of stereolithography using in-process techniques. Rapid Prototyp J 3(1):20–31

50. Wang XC, Kruth JP (2000) A simulation model for direct selective laser sintering of metal powders. Computational Techniques for

Materials, Composites and Composite Structures, Civil-Comp, Edinburgh, pp 57–71

51. Chen T, Zhang Y (2004) Numerical simulation of two-dimensional melting and resolidification of a two-component metal powder layer in selective laser sintering process. Numer Heat Tran Part A 46: 633–649

52. Hu D, Kovacevic R (2003) Sensing, modeling and control for laser-based additive manufacturing. Int J Mach Tools Manuf 43(1):51–60

53. Dong L, Makradi A, Ahzi S, Remond Y (2009) Three-dimensional transient finite element analysis of the selective laser sintering process. J Mater Process Technol 209(2):700–706

54. Chen T, Zhang Y (2006) A partial shrinkage model for selective laser sintering of a two-component metal powder layer. Int J Heat Mass Transf 49:1489–1492

55. Toyserkani E, Khajepour A, Corbin S (2004) 3-D finite element modeling of laser cladding by powder injection: effects of laser pulse shaping on the process. Opt Lasers Eng 41:849–867

56. Muller P, Mognol P, Hascoet JY (2013) Modeling and control of a direct laser powder deposition process for functionally graded materials (FGM) parts manufacturing. J Mater Process Technol 213(5): 685–692

57. Crockett RS, Calvert PD (1996) The liquid-to-solid transition in stereodeposition techniques. In: Solid freeform fabrication proceedings. University of Texas at Austin, Austin, pp 257–264

58. Anitha R, Arunachalam S, Radhakrishan P (2001) Critical parameters influencing the quality if prototypes in fused deposition modeling. J Mater Process Technol 118(1–3):385–388

59. Raghunath N, Pandey PM (2007) Improving accuracy through shrinkage modelling by using Taguchi method in selective laser sintering. Int J Mach Tools Manuf 47:985–995

60. Michaleris P (2014) Modeling metal deposition in heat transfer analyses of additive manufacturing processes. Finite Elem Anal Des 86:51–60

61. Strano G, Hao L, Everson RM, Evans KE (2013) Surface roughness analysis, modelling and prediction in selective laser melting. J Mater Process Technol 213(4):589–597

62. Fan Z, Liou F (2012) Numerical modeling of the additive manufacturing (AM) processes of titanium alloy, from "Titanium Alloys—Towards Achieving Enhanced Properties for Diversified Applications". InTech, Missouri University of Science and Technology

63. Matsumoto M, Shiomi M, Osakada K, Abe F (2002) Finite element analysis of single layer forming on metallic powder bed in rapid prototyping by selective laser processing. Int J Mach Tools Manuf 42(1):61–67

64. Vasinonta A, Beuth J, Griffith M (2000) Process maps for controlling residual stress and melt pool size in laser-based SFF processes. In Solid Freeform Fabrication Proceedings, University of Texas at Austin, Austin, pp 200–208

65. Curodeau A (1995) Three dimensional printing of ceramic molds with accurate surface macro-textures for investment casting of orthopaedic implants. Thesis (Ph. D.)-Massachusetts Institute of Technology, Dept. of Mechanical Engineering

66. Crespo A, Deus AM, Vilar R (2006) Finite element analysis of laser powder deposition of titanium. Proceedings of ICALEO 2006, Scottsdale, Arizona, Laser Institute of America, Orlando, Florida, pp 1016–1021

67. Costa L, Deus AM, Reti T, Vilar R (2002) Simulation of layer overlap tempering in steel parts produced by laser cladding. Proceedings of the RPD 2002, Marinha Grande

68. Bellini A, Güçeri S, Bertoldi M (2004) Liquefier dynamics in fused deposition. J Manuf Sci Eng Trans ASME 126:237–246

69. Venkataraman N, Rangarajan S, Matthewson MJ, Harper B, Safari A, Danforth SC, Wu G, Langrana N, Guceri S, Yardimci A (2002) Feedstock material property-process relationships in fused deposition of ceramics (FDC). Rapid Prototyp J 6:244–252

70. Yardimci MA, Hattori T, Guceri SI, Danforth SC (1997) Thermal analysis of fused deposition. In: Solid freeform fabrication proceedings. University of Texas at Austin, Austin

71. Agarwala MK, Jamalabad VR, Langrana NA, Safari A, Whalen PJ, Danforth SC (1996) Structural quality of parts processed by fused deposition. Rapid Prototyp J 2:4–19

72. Ramanath HS, Chua CK, Leong KF, Shah KD (2008) Melt flow behaviour of poly-epsilon-caprolactone in fused deposition modeling. J Mater Sci-Mater Med 19:2541–2550

73. Zhang Y, Chou YK (2006) Three-dimensional finite element analysis simulations of the fused deposition modelling process. J Eng Manuf 220(10):1663–1671

74. Zhang Y, Chou YK (2008) A parameter study of part distortions in FDM using 3D FEA. J Eng Manuf 222:959–967

75. Mostafa N, Syed HM, Igor S, Andrew G (2009) A study of melt flow analysis of an ABS-iron composite in fused deposition modelling process. Tsinghua Sci Technol 14:29–37

76. Ji LB, Zhou TR (2010) Finite element simulation of temperature field in fused deposition modeling. Manuf Sci Eng 97/101:2585–2588

77. Martínez J, Diéguez JL, Ares E, Pereira A, Hernández P, Pérez JA (2013) Comparative between FEM models for FDM parts and their approach to a real mechanical behaviour. Procedia Eng 63:878–884

78. Nikzad M, Hasan Masood S, Sbarski I, Groth A (2009) Thermo-mechanical properties of a highly filled polymeric composites for fused deposition modeling. Tsinghua Sci Technol 14:29–37

79. Venkataraman N, Rangarajan S, Matthewson MJ, Safari A, DanforthSC, Yardimci A (1999) Mechanical and rheological properties of feedstock material for fused deposition of ceramics and metals (FDC and FDMet) and their relationship to process performance. In Solid Freeform Fabrication Proceedings, University of Texas at Austin, Austin, pp 351–360

80. Sood AK, Ohdar RK, Mahapatra SS (2012) Experimental investigation and empirical modelling of FDM process for compressive strength improvement. J Adv Res 3(1):81–90

81. Jee HJ, Sachs E (2000) A visual simulation technique for 3D printing. Adv Eng Softw 31:97–106

82. Sachs E, Vezzetti E (2005) Numerical simulation of deposition process for a new 3DP printhead design. J Mater Process Technol 161:509–515

83. Gockel J, Beuth J, Taminger K (2014) Integrated control of solidification microstructure and melt pool dimensionsin electron beam wire feed additive manufacturing of Ti-6Al-4V. Addit Manuf 1–4: 119–126

84. Shen N, Chou K (2012) Numerical thermal analysis in electron beam additive manufacturing with preheating effects. Proceedings of the 23rd annual international solid freeform fabrication symposium, pp 774–784

85. Shen N, Chou YK (2012) Thermal modeling of electron beam additive manufacturing process—powder sintering effects. Proc. the 7th ASME 2012 International Manufacturing Science and Engineering Conference, pp 287–295

86. Markl M, Ammer R, Ljungblad U, Ruede U, Koerner C (2013) Electron beam absorption algorithms for electron beam melting processes simulated by a three–dimensional thermal free surface lattice Boltzmann method in a distributed and parallel environment. Procedia Comput Sci 18:2127–2136

87. Ammer R, Markl M, Ljungblad U, Koerner C, Róde U (2014) Simulating fast electron beam melting with a parallel thermal free surface lattice Boltzmann method. Comput Math Appl 67(2):318–330

88. Chryssolouris G, Kotselis J, Koutzampoikidis P, Zannis S, Mourtzis D (1999) Dimensional accuracy modeling of stereolithography parts, 32nd CIRP International Seminar on Manufacturing Systems, Leuven, pp 213–218

89. Wiedemann B, Dusel KH, Eschl J (1995) Influence of the polymerization dynamics of stereolithography resins on accuracy.

Proceeding of the 6th International Conference on RP University of Dayton, Ohio

90. NaraharaH, Tamaka F, Kishimani T, Igarashi S, Saito K (1997) Reaction heat effect on initial linear shrinkage of stereolithography resins. Proceedings of Solid Freeform Fabrication Symposium, pp 733–740

91. Giannatsis J, Deboussis V, Laios L (2001) A study of the build-time estimation problem for stereolithography systems. Robot Comput Integr Manuf 17:295–304

92. Liu FR, Zhang Q, Zhou WP, Zhao JJ, Chen JM (2012) Micro scale 3D FEM simulation on thermal evolution within the porous structure in selective laser sintering. J Mater Process Technol 212(10): 2058–2065

93. Khairallah SA, Anderson A (2014) Mesoscopic simulation model of selective laser melting of stainless steel powder. J Mater Process Technol 214(11):2627–2636

94. Kolossov S, Boillat E, Glardon R, Fischer P, Locher M (2004) 3D FE simulation for temperature evolution in the selective laser sintering process. Int J Mach Tools Manuf 44(2–3): 117–123

95. Costa L, Vilar R, Reti T, Deus AM (2005) Rapid tooling by laser powder deposition: process simulation using finite element analysis. Acta Mater 53:3987–3999

96. Stavropoulos P, Chantzis D, Doukas C, Papacharalampopoulos A, Chryssolouris G (2013) Monitoring and control of manufacturing processes: a review. Procedia CIRP, 14th CIRP Conference on Modelling of Machining Operations, Turin

97. Yu C, Smurov I (2010) On-line temperature monitoring in selective laser sintering/melting. Phys Procedia Part B 5:515–521

98. Kwon KS, Choi YS, Lee DY, Kim JS, Kim DS (2012) Low-cost and high speed monitoring system for a multi-nozzle piezo inkjet head. Sensors Actuators A 180:154–165